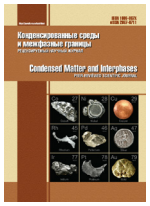

ISSN 1606-867X (Print)
ISSN 2687-0711 (Online)
Condensed Matter and Interphases
Kondensirovannye Sredy i Mezhfaznye Granitsy
https://journals.vsu.ru/kcmf/

Original articles

Research article
https://doi.org/10.17308/kcmf.2023.25/10975

Formation during glycine-nitrate combustion and magnetic properties of $YFe_{1-x}Ni_xO_3$ nanoparticles

E. I. Lisunova[1], N. S. Perov[2], V. O. Mittova[3], Bui Xuan Vuong[4], Nguyen Anh Tien[5], B. V. Sladkopevtsev[1]✉, Yu. A. Alekhina[2], V. F. Kostryukov[1], I. Ya. Mittova[1]

[1]Voronezh State University,
1 Universitetskaya pl., Voronezh, 394018, Russian Federation

[2]Lomonosov Moscow State University
1, building 2 Leninskie Gory, Moscow 119991, Russian Federation

[3]Teaching University Geomedi
4 st. King Solomon II str. 0114, Tbilisi, Georgia

[4]Faculty of Natural Sciences Education, Saigon University,
273 An Duong Vuong St., Ward 3, District 5, Ho Chi Minh City, Vietnam

[5]Faculty of Chemistry, Ho Chi Minh City University of Education,
Ho Chi Minh City 700000, Vietnam

Abstract

The synthesis of FeO_3 and $YFe_{1-x}Ni_xO_3$ (x = 0.1; 0.15; 0.2; 0.3; 0.5) nanocrystals was performed under the conditions of a self-propagating wave of glycine-nitrate combustion and their characterization and determination of the effect of Ni^{2+} doping of yttrium ferrite on the magnetic properties of nanopowders.

The technology for the synthesis of yttrium orthoferrite nanoparticles (with and without doping with Ni^{2+} ions) by the glycine-nitrate combustion method at a ratio of G/N = 1 and 1.5 without adding a gelling agent to the reaction mixture and using ethylene glycol/glycerol is described. For the characterization of nanopowders based on $YFeO_3$, the following were determined: phase composition and crystal structure (X-ray diffraction (XRD) method); size and structure of nanocrystal particles (transmission electron microscopy (TEM)); elemental composition of the samples (local X-ray spectral microanalysis (LXSMA)); magnetic characteristics (field dependences of specific magnetization).

Thermal annealing of the synthesized samples at 800°C for 60 min led to the formation of the o-$YFeO_3$ main phase. Undoped samples of yttrium orthoferrite were characterized by a particle diameter in the range of 5-185 nm, depending on the gelling agent used. $YFe_{1-x}Ni_xO_3$ particles had a predominantly round shape with a size of 24 to 31 nm; the non-monotonic dependence of the average particle diameter on the dopant content was revealed: as the amount of dopant added increased, the average crystallite size tended to decrease. Nanopowders of undoped yttrium orthoferrite exhibit antiferromagnetic behaviour of magnetic susceptibility with temperature. The change in the magnetic properties of the nickel-doped $YFeO_3$ nanocrystalline powders was due to the incorporation of Ni^{2+} into the Fe^{3+}position, which led to the formation of a material with more pronounced soft magnetic properties at a substitution degree of 0.1. Samples with high degrees of substitution (x = 0.15 and 0.3) were also characterized by paramagnetic behaviour at temperatures above 100 K.

Keywords: Nanocrystals, Yttrium orthoferrite, Nickel, Doping, Glycine-nitrate combustion

Funding: The reported study was funded by RFBR, project number 20-33-90048 Aspiranty.

Acknowledgements: The studies were carried out using the equipment of the Centre for the Collective Use of Scientific Equipment of Voronezh State University, as well as on the facilities of the Department of Magnetism of the Lomonosov Moscow State University, acquired with the aid of the Development Program for the Lomonosov Moscow State University.

✉ Boris V. Sladkopevtsev, e-mail: dp-kmins@yandex.ru

For citation: Lisunova E. I., Perov N. S., Mittova V. O., Vuong B. X., Nguyen A. T., Sladkopevtsev B. V., Alekhina Yu. A., Kostryukov V. F., Mittova I. Ya. Formation during glycine-nitrate combustion and magnetic properties of $YFe_{1-x}Ni_xO_3$ nanoparticles. *Condensed Matter and Interphases*. 2023;25(1): 61–71. https://doi.org/10.17308/kcmf.2023.25/10975

Для цитирования: Лисунова Е. И., Перов Н. С., Миттова В. О., Буи Х. В., Нгуен А.Т., Сладкопевцев Б. В., Алехина Ю. А., Кострюков В. Ф., Миттова И. Я. Формирование в процессе глицин-нитратного горения и магнитные свойства наночастиц $YFe_{1-x}Ni_xO_3$. *Конденсированные среды и межфазные границы*. 2023;25(1): 61–71. https://doi.org/10.17308/kcmf.2023.25/10975

1. Introduction

The preparation of nanocrystalline perovskite-like orthoferrites of rare-earth elements (REE), as well as solid solutions and composite materials based on them, is now one of the most intensively developing areas of research of material science [1–5]. Interest in this class of inorganic substances is mainly due to the possibility of using the properties of REE orthoferrites as multiferroics, which are practically important for use in data storage, gas sensors, and fuel cells [6–8].

One of the brightest representatives of this class is $YFeO_3$, which possesses a variety of important properties (multiferroic, semiconductor, photocatalyst in the visible light region, etc.) and is complemented by the economic feasibility of using materials based on it due to the highest prevalence of yttrium among the entire series of rare earth elements [9–11]. $YFeO_3$ nanopowders can be obtained by co-deposition [12], hydrothermal synthesis [13], sol-gel technology, and other methods [14, 15].

The tendency of nanoparticles to agglomerate is an important factor affecting the size of clusters in a solution and, hence, their physicochemical properties [15–18]. Recently, the method for obtaining complex oxide systems in a combustion wave and, in particular, glycine-nitrate combustion method (GNC) has been actively used. GNC allows to ensure high chemical homogeneity of substances by mixing the initial components at the molecular level at relatively low temperatures [19–22]. The main advantage of this method is the achievement of a narrow particle size distribution, therefore GNC is actively used for the synthesis of nanocrystalline $YFeO_3$ [23, 24]. However, the influence of gelling agents on the process of formation of yttrium orthoferrite nanocrystals (with and without doping) under the conditions of a self-propagating wave of glycine-nitrate combustion, their size, structure, and magnetic properties of the resulting composition still remains unexplored.

Particular attention is paid to the study of the magnetic properties of yttrium orthoferrite doped with doubly charged cations [25 – 28]. For example, it was shown in [29] that the doping of $YFeO_3$ with cobalt provides an increase in the magnetic permeability of the material and a broadening of the hysteresis loop, caused by an increase in the angularity of the magnetic moments of atoms in antiferromagnets. Therefore, the cation of the transition element Ni^{2+} with defective *d*–shell was chosen for the doping of yttrium ferrite. Due to the similarity in physicochemical properties and dimensional parameters according to the system of Shannon radii ($r(Ni^{2+})$ = 0.69 Å), nickel, most probably, should occupy the positions of iron in the ferrite lattice ($r(Fe^{3+})$ = 0.65 Å) [30].

In this regard, the aim of the study was the synthesis of $YFeO_3$ and $YFe_{1x}Ni_xO_3$ nanocrystals under the conditions of a self-propagating wave of glycine-nitrate combustion, their characterization and determination of the influence of doping of yttrium ferrite with Ni^{2+} on the magnetic properties of nanopowders.

2. Experimental

The starting materials were pure iron (III) and yttrium nitrates – $Fe(NO_3)_3 \cdot 9H_2O$ (pure) and $Y(NO_3)_3 \cdot 6H_2O$ (chemically pure), glycine (aminoacetic acid) $C_2H_5NO_2$ (analytical grade), the amount of which in relation to metal nitrates G/N varied from 1 to 1.5. In the general case, polyatomic alcohols are used as gelling agents. Due to the use of polyatomic alcohols the polyesterification of chelates occurs; in this study, chemically pure glycerol $C_3H_5(OH)_3$ and ethylene glycol $C_2H_4(OH)_2$, were used as gelling agents. As a result, a uniform distribution of Y (III) and Fe (III) metal ions is achieved in the initial precursor, during subsequent heat treatment of the precursor a complex oxide powder, corresponding to the main phase of $YFeO_3$ is formed.

The procedure for the synthesis of nanocrystals was as follows. The $Y(NO_3)_3 \cdot 6H_2O$, $Fe(NO_3)_3 \cdot 9H_2O$

and $C_2H_5NO_2$ were dissolved in 200 ml of distilled water. In addition to glycine, ethylene glycol or glycerol was added to the solution of metal nitrates. The amount of gelling agent was changed depending on the main components, G/N = 1 and G/N = 1.5, respectively. The boiling was performed for 120 minutes. The resulting gel was subjected to thermal heating, as a result of which the self-sustaining exothermic reaction involving glycine (aminoacetic acid) developed. The final product (in powder form) was annealed in a muffle furnace at 800°C for 60 minutes. These thermal annealing parameters were chosen based on our previous results on the co-deposition of nickel-doped $YFeO_3$ nanocrystals [31]. It was also shown that under these conditions, the formation of a single-phase yttrium orthoferrite product with a perovskite structure and particle sizes up to 160 nm occurs. A further increase in the temperature and time of annealing is undesirable, since it leads to coarsening of particles and their agglomeration.

The phase composition and crystal structure of the synthesized samples were determined by X-ray diffraction (XRD, diffractometer Thermo ARL X'tra (CuK_α radiation, $\lambda = 0.154018$ nm, $2\theta = 20–70^o$, step = 0.02°). The particle size was determined using the transmission electron microscopy (TEM, Carl Zeiss LIBRA 120). For the determination of the elemental composition of the samples, electron probe X-ray microanalysis (EPMA, JEOL-6580LV scanning electron microscope with an INCA 250 energy-dispersive microanalysis system) was used.

Measurements of the temperature dependences of the magnetic susceptibility up to helium temperatures were carried out using the PPMS (Physical Properties Measurement System). The same installation was used to measure the hysteresis loops of sample 5 (see below) with ferrimagnetic ordering in fields up to 6.4 MA/m. The magnetic properties of the remaining samples were measured using LakeShore vibrating magnetometer model 7407. The samples were sealed in polyethylene capsules about 4x4 mm in size and laminated for the prevention of the movement of powder particles during measurements. The capsules were fixed on the magnetometer holder with a Teflon tape. The magnetic field during measurements was applied in the plane of the capsule. The measurements were carried out in a cryostat at temperatures of 100 and 300 K.

3. Results and discussion

As can be seen from the XRD data (Fig. 1) thermal annealing at a temperature of 800°C for 60 minutes of undoped samples, synthesized under the conditions of glycine-nitrate combustion with the ratio G/N = 1 without adding a gelling agent to the reaction mixture (diffraction pattern 1) and with the addition of ethylene glycol at ratios G/N = 1 and G/N = 1.5 (diffraction patterns 2 and 3), led to the formation of yttrium orthoferrite powders. At the same time, for both G/N = 1 and for G/N = 1.5 using glycerol as a gelling agent, in addition to the main $YFeO_3$ phase (cards No.: 48-0529 and 39-1489), the presence of Y_2O_3 impurities (card No: 20-1412) was established, as can be seen from diffraction patterns 4 and 5 in Figs. 1 (see Table 1).

On diffraction patterns of yttrium ferrite samples (Fig. 2, beginning of numbering in Fig. 1, diffraction patterns 6 and 7), doped with Ni^{2+}, under conditions of glycine-nitrate combustion at G/N = 1 without the use of gelling agents, followed by thermal annealing at 800 °C for 60 minutes, peaks of the main yttrium orthoferrite phase were observed (cards No.: 48-0529 and 39-1489). In addition to reflections of the main phase, diffraction patterns No. 6 and 7 contain one impurity peak of yttrium oxide with insignificant intensity (card No. 20-1412). When glycerol (Fig. 2, diffraction patterns No. 8 and No. 9) and ethylene glycol (Fig. 2, diffraction patterns No. 10 and No. 11) were used, the presence of the main phase of yttrium orthoferrite and an insignificant number of peaks of Y_2O_3 oxide was observed (Fig. 2).

The determination of the particle size of $YFe_{1-x}Ni_xO_3$ nanopowders (x = 0.1; 0.15; 0.2; 0.3; 0.5), based on the broadening of X-ray diffraction lines (calculated using Scherrer equation) and transmission electron microscopy, provided the following results (Table 2). The calculation using Scherrer equation (XRD) showed that with an increase x from 0.1 to 0.3 D_{av} of nanocrystals varies from 27±2 nm to 47±4 nm, respectively (XRD). As follows from the TEM data, nickel-doped yttrium ferrite nanoparticles with a nominal degree of doping x = 0.15 at G/N = 1.5 with the addition

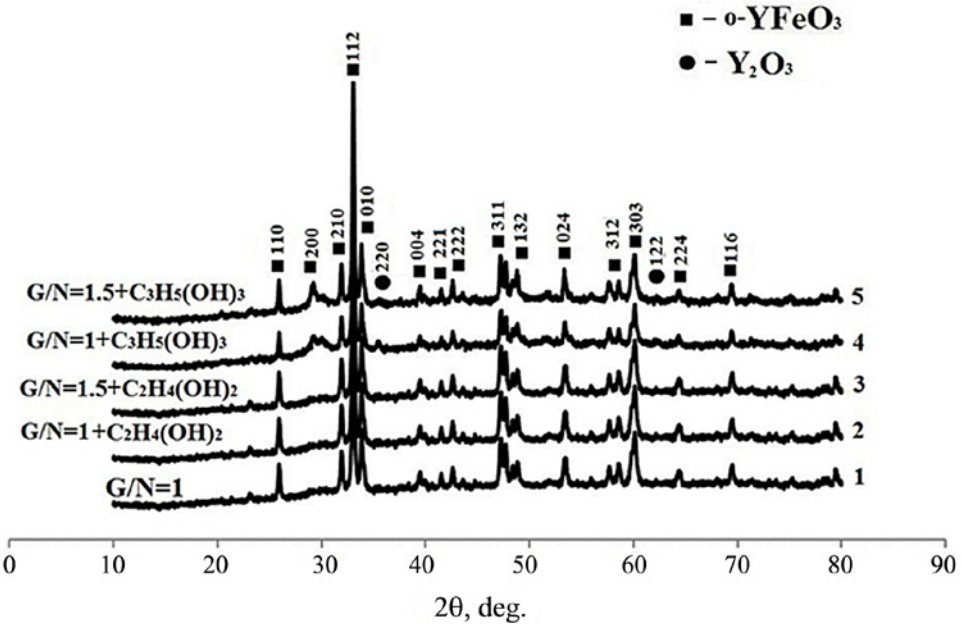

Fig. 1. X-ray diffraction patterns of $YFeO_3$ powders, obtained by the glycine-nitrate method, with a different ratio of G/N components and various gelling agents after thermal annealing at 800°C, 60 min: *1* – G/N = 1 without the addition of a gelling agent; *2*, *3* – G/N = 1 and 1.5, respectively, gelling agent – ethylene glycol $C_2H_4(OH)_2$; *4*, *5* – G/N = 1 and 1.5, gelling agent – glycerol $C_3H_5(OH)_3$

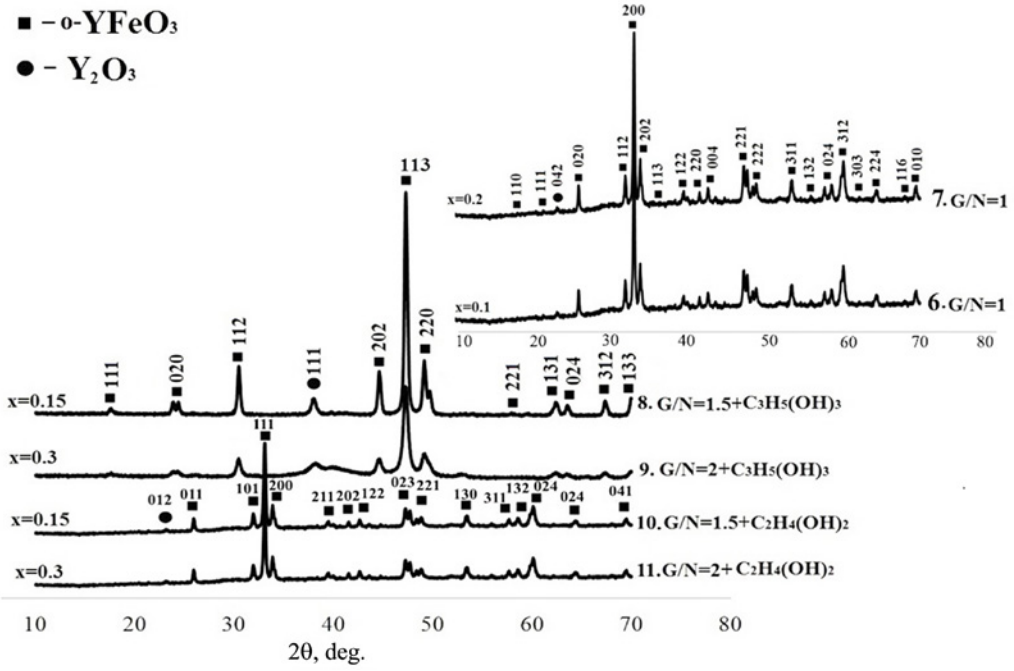

Fig. 2. X-ray diffraction patterns of powders thermally annealed at 800°C, 60 min: *6* – $YFe_{1-x}Ni_xO_3$ (x = 0.1) at G/N = 1 without the addition of a gelling agent; *7* – $YFe_{1-x}Ni_xO_3$ (x = 0.2) at G/N = 1 without the addition of a gelling agent; *8* – $YFe_{1-x}Ni_xO_3$ (x = 0.15) at G/N = 1.5, gelling agent – glycerol $C_3H_5(OH)_3$; *9* – $YFe_{1-x}Ni_xO_3$ (x = 0.3) at G/N = 2, gelling agent – glycerol $C_3H_5(OH)_3$; *10* – $YFe_{1-x}Ni_xO_3$ (x = 0.15) at G/N = 1.5, gelling agent – ethylene glycol $C_2H_4(OH)_2$; *11* – $YFe_{1-x}Ni_xO_3$ (x = 0.3) at G/N = 2, gelling agent – ethylene glycol $C_2H_4(OH)_2$

Table 1. Results of X-ray phase analysis of $YFeO_3$ and $YFe_{1-x}Ni_xO_3$nanopowders

№	Composition	G/N	Gelling agent	Additional phase
1	$YFeO_3$	1	–	–
2	$YFeO_3$	1	$C_2H_4(OH)_2$	–
3	$YFeO_3$	1.5	$C_2H_4(OH)_2$	–
4	$YFeO_3$	1	$C_3H_5(OH)_3$	Y_2O_3
5	$YFeO_3$	1.5	$C_3H_5(OH)_3$	Y_2O_3
6	$YFe_{0.9}Ni_{0.1}O_3$	1	–	Y_2O_3
7	$YFe_{0.8}Ni_{0.2}O_3$	1	–	Y_2O_3
8	$YFe_{0.85}Ni_{0.15}O_3$	1.5	$C_3H_5(OH)_3$	Y_2O_3
9	$YFe_{0.7}Ni_{0.3}O_3$	2	$C_3H_5(OH)_3$	Y_2O_3
10	$YFe_{0.85}Ni_{0.15}O_3$	1.5	$C_2H_4(OH)_2$	Y_2O_3
11	$YFe_{0.7}Ni_{0.3}O_3$	2	$C_2H_4(OH)_2$	Y_2O_3

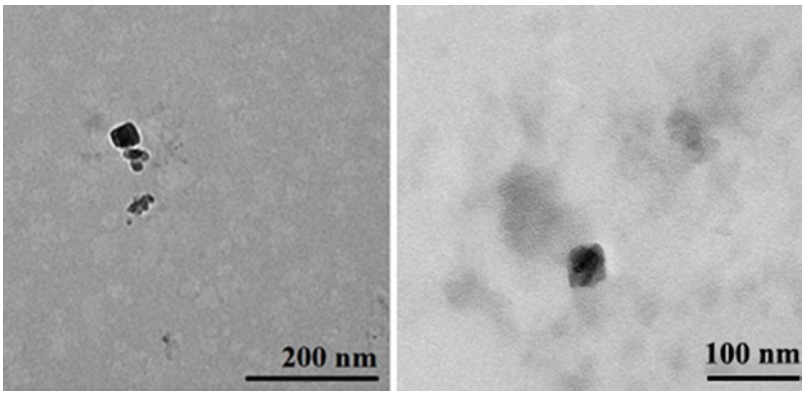

a b

Fig. 3. TEM images (a, b) of $YFe_{1-x}Ni_xO_3$ powder (x = 0.15), in the ratio G/N = 1.5, gelling agent – $C_2H_4(OH)_2$ (a, Sample No. 10) and $C_3H_5(OH)_3$ (b, sample No. 8), annealing – 800°C, 60 min

of ethylene glycol (Fig. 3a) and glycerol (Fig. 3b) were characterized predominantly by a spherical shape, their diameter was in the range from 4 to 50 nm (Fig. 3).

As can be seen from Table 2 the data obtained show the non-monotonic nature of the dependence D_{av} from the content of the dopant. As the amount of added dopant increased, the average crystallite size tends to decrease; such a decrease may be caused by the peculiarities of the chemical structure of gelling agents (ethylene glycol/glycerol).

The results of the study of the elemental composition by the local X-ray spectral microanalysis are shown in Table 3.

Determination of the elemental composition of the samples showed that the actual content of each element in them is quite close to their nominal composition (Table 4).

The field dependences of the magnetization of undoped samples synthesized without the use of a gelling agent and with the addition of ethylene glycol are shown in Figs. 4–5. Samples in a field of 1270 kA/m at T = 100 K (Fig. 4a) and 300 K (Fig. 4b) do not reach magnetic saturation (flip transition). The field dependences of the specific magnetization are straight lines (the noise on the dependences was primarily associated with the smallness of measured magnetization values), the maximum measured values of the magnetization for these samples in a field of 1270 kA/m were in the range of 0.25–0.36 A m^2/kg at a temperature of 100 K and 0.12–0.30 A m^2/kg at a temperature of 300 K (Table 5). The magnetic properties of the samples were comparable to those for the pure $YFeO_3$ phase, synthesized by the deposition method [32]. The specific magnetization of pure $YFeO_3$ phase in a magnetic field of the same

Table 2. Average diameter of $YFe_{1-x}Ni_xO$ nanocrystals (x = 0.1; 0.15; 0.2; 0.3) after annealing at 800 °C for 60 min

Method of determination	D_{av}, nm					
	sample № 6 (x = 0.1)	sample № 7 (x = 0.2)	sample № 8 (x = 0.15)	sample № 10 (x = 0.15)	sample № 9 (x = 0.3)	sample № 11 (x = 0.3)
XRD	27±2	40±4	24±2	40±4	47±4	26±2
TEM	31±3	26±2	17±5	31±2	24±9	28±5

Table 3 Results of X-ray microanalysis and the determination error of the content of elements in $YFe_{1-x}Ni_xO_3$ samples obtained by glycine-nitrate combustion, after thermal annealing at 800 °C, 60 min

Sample №	Nominal composition of samples	Elemental composition, at %				
	x	Y	Ni	Fe	O	C
6	0.1	15.9±1.8	0.8 ±0.1	11.9±0.6	55.0±3.4	16.0±1.0
7	0.2	13.1±1.6	2.3±0.2	10.9±0.6	58.6±3.8	15.1±1.0
8	0.15	10.1±1.4	3.1±0.2	6.8±0.4	63.0±4.5	17.0±1.2
9	0.3	10.1±1.4	3.1±0.2	6.8±0.4	61.0±4.5	19.0±1.2
10	0.15	18.4±1.8	1.1±0.1	14.2±0.6	50.9±2.8	15.3±0.9
11	0.3	18.4±1.8	1.3±0.1	14.2±0.6	50.8±2.8	15.3±0.9

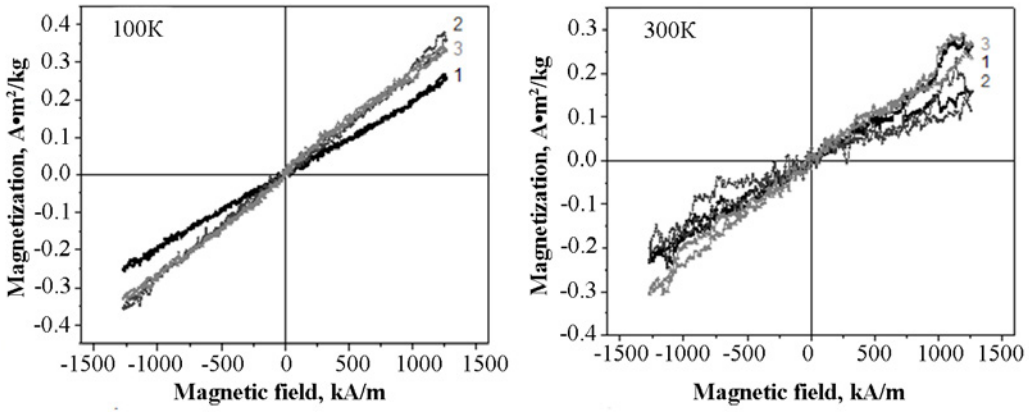

a b

Fig. 4. Hysteresis loops at a) 100 K and b) 300 K of $YFeO_3$ samples (annealing at 800°C, 60 min) synthesized at component ratios: G/N = 1 without the addition of a gelling agent (*1*) and G/N = 1 and 1.5 with the addition of ethylene glycol (*2*, *3*)

value was J = 0.242 A m²/kg. In the given range of magnetic fields and temperatures, the material exhibits paramagnetic behaviour. In this case, the temperature dependences of the magnetization indicate the existence of an antiferromagnetic type of ordering at low temperatures. The linear approximation of the curve section crosses the abscissa axis in the region of negative values, which indicates the presence of an antiferromagnetic type (Fig. 5b). The maximum of the direct dependence of the susceptibility, corresponding to the Neel temperature, can be observed at temperatures below 2 K, however, the existence of local ordering can be observed up to 100 K.

According to the literature data, yttrium ferrite is a weak ferromagnet, which demonstrates the phenomenon of spin reorientation - rotation of the antiferromagnetism axis under the action of a magnetic field [15]. The magnetic properties of undoped sample 5, synthesized with the addition of glycerol as a gelling agent at G/N = 1.5, in a wide range of magnetic fields demonstrated the presence of a wide hysteresis loop, which is characteristic of materials with an antiferromagnetic type of ordering with an

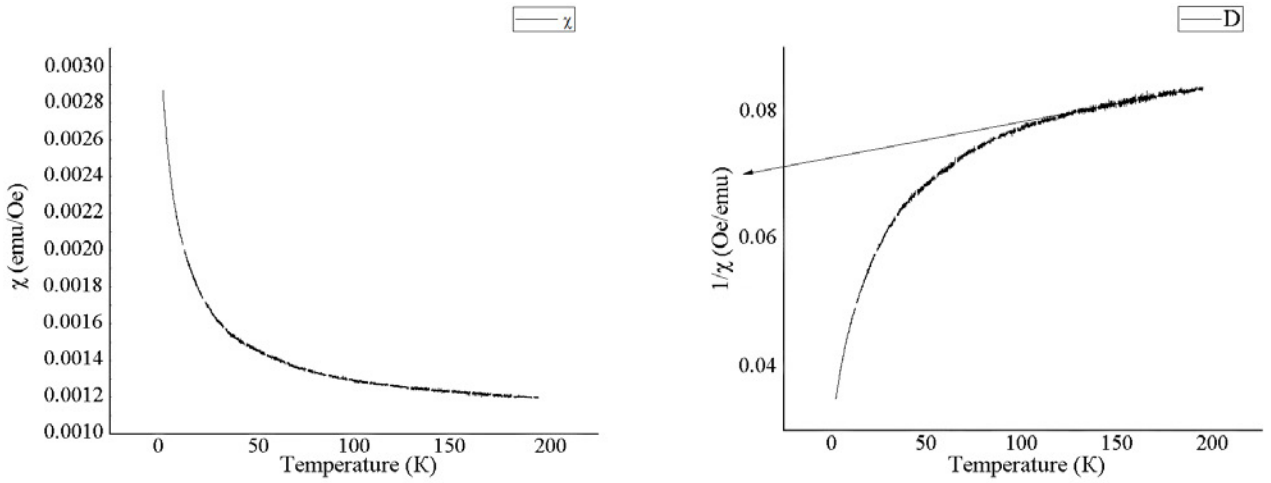

a b

Fig. 5. Temperature dependence of magnetic susceptibility (a) and inverse susceptibility (b) for sample 1 from Table 5 (for samples 2 and 3, the dependences were similar)

uncompensated magnetic moment (Fig. 6). At 2 K, the field dependences of the magnetization also show a waisted hysteresis loop, which indicates a more expressed spin reorientation phenomenon [15]. It should also be noted that for the samples synthesized using glycerol, the formation of an impurity phase of yttrium oxide was observed.

The hysteresis of the field dependences was also observed for a sample of yttrium orthoferrite with a low degree of nickel doping. For a sample with a degree of substitution x = 0.1 at G/N = 1 without the addition of a gelling agent to the reaction system, hysteresis behaviour, indicating the presence of an uncompensated magnetic moment was observed in the range of magnetic fields up to 1270 kA/m (Fig. 7, Table 6). In this case, in the region of magnetic fields with a strength of about 1000 kA/m, an inflection in the field dependence of the magnetization was observed, the appearance of which may indicate the onset of the spin reorientation process, but the process itself can be observed only when stronger magnetic fields were applied. The absence of magnetic saturation of the samples in the presented range of magnetic fields also should be noted. At the same time, the coercive force in the given partial cycles was about 50–80 kA/m (both at 300 K and at 100 K), which is an order of magnitude lower than the

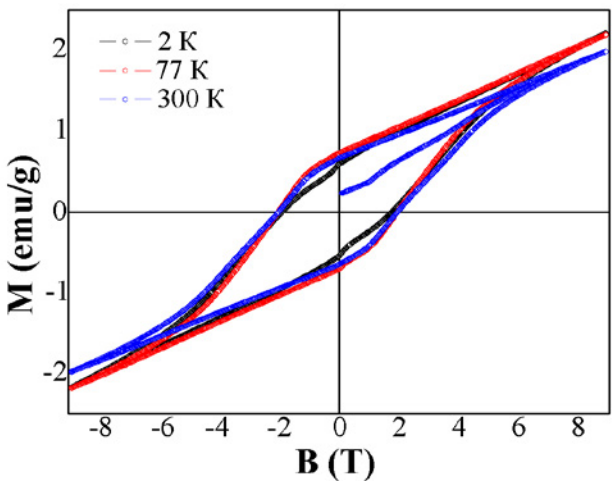

Fig. 6. Hysteresis loops of sample 5 synthesized with glycerol at different temperatures. At 2 K (black line) there was a tendency to transition to the antiferromagnetic state

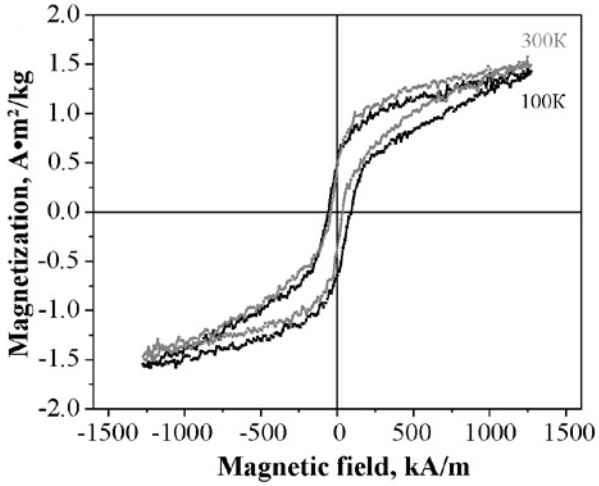

Fig. 7. Hysteresis loops of sample 6 with nominal composition $YFe_{0.9}Ni_{0.1}O_3$ (annealing at 800 °C, 60 min) at G/N = 1 without the addition of a gelling agent

coercive force of the undoped sample measured under similar conditions (about 520–550 kA/m). Thus, the doping of yttrium ferrite with nickel to a small extent allows obtaining materials with a softer magnetic behaviour of the uncompensated magnetic moment and smaller spin reorientation fields.

For samples with high degrees of substitution (x = 0.15, x = 0.3) and obtained using glycerol and ethylene glycol as gelling agents in the range of magnetic fields up to 1270 kA/m, paramagnetic behaviour was observed at temperatures above 100 K with a susceptibility of about 10^{-5}-10^{-6} (Fig. 8).

Other $YFe_{1-x}Ni_xO_3$ (x = 0.15 and 0.3) samples No. 8 and 9, synthesized using glycerol as a gelling agent in the ratio G/N = 1.5 and 2, respectively, as well as $YFe_{1-x}Ni_xO_3$ (x = 0.15 and 0.3) samples No. 10 and 11, obtained with the addition of ethylene glycol in the same ratio G/N = 1.5 and 2, demonstrated paramagnetic behaviour.

Thus, during the formation of yttrium orthoferrite nanopowders (with and without

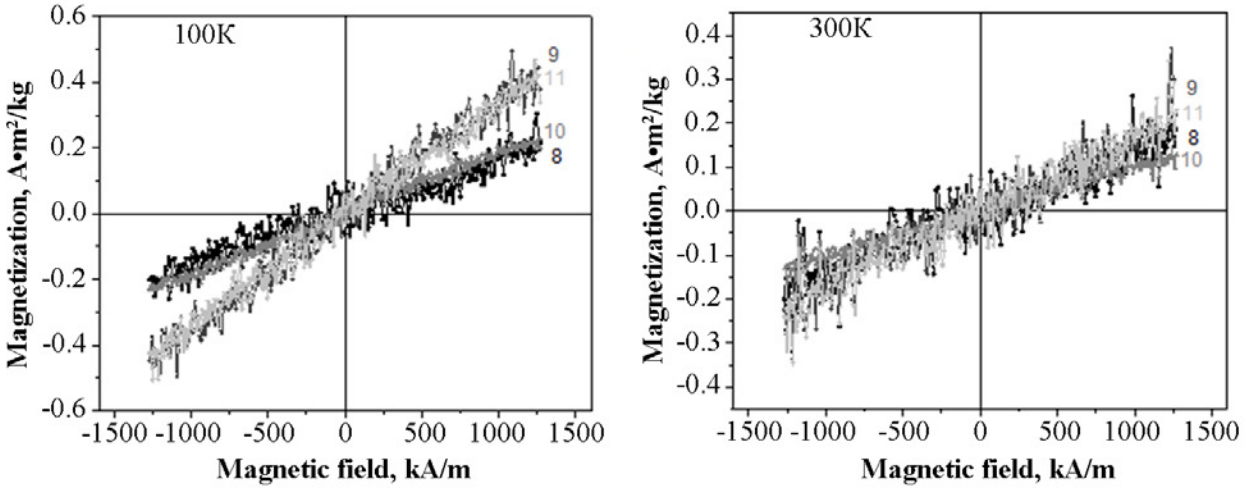

a b

Fig. 8. Field dependences of the magnetization for samples thermally annealed at 800°C, 60 min: *8* – nominal composition $YFe_{0.85}Ni_{0.15}O_3$ at G/N = 1 with the addition of glycerol, *9* – nominal composition $YFe_{0.7}Ni_{0.3}O_3$ at G/N = 2 with the addition of glycerol, *10* – nominal composition $YFe_{0.85}Ni_{0.15}O_3$ at G/N = 1.5 with the addition of ethylene glycol, *11* – nominal composition $YFe_{0.7}Ni_{0.3}O_3$ at G/N = 2 with the addition of ethylene glycol

Table 4 Results of X-ray microanalysis for $YFe_{1-x}Ni_xO_3$samples obtained by glycine-nitrate combustion after thermal annealing in 800 °C mode, 60 min

Sample №	G/N	Gelling agent	x	Nominal composition	Real composition of samples
6	1	-	0.1	$YFe_{0.9}Ni_{0.1}O_3$	$YFe_{0.92}Ni_{0.08}O_3$
7	2	-	0.2	$YFe_{0.8}Ni_{0.2}O_3$	$YFe_{0.83}Ni_{0.17}O_3$
8	1.5	$C_3H_5(OH)_3$	0.15	$YFe_{0.85}Ni_{0.15}O_3$	$YFe_{0.75}Ni_{0.25}O_3$
9	2	$C_3H_5(OH)_3$	0.3	$YFe_{0.7}Ni_{0.3}O_3$	$YFe_{0.69}Ni_{0.31}O_3$
10	1.5	$C_2H_4(OH)_2$	0.15	$YFe_{0.85}Ni_{0.15}O_3$	$YFe_{0.79}Ni_{0.21}O_3$
11	2	$C_2H_4(OH)_2$	0.3	$YFe_{0.7}Ni_{0.3}O_3$	$YFe_{0.73}Ni_{0.27}O_3$

Table 5 Magnetic characteristics of undoped $YFeO_3$ nanopowders (annealing at 800°C, 60 min), measured at 100 and 300 K

№	G/N	Gelling agents	Particle size (TEM), nm	J(100K), A·m²/kg	J(300K), A·m²/kg
1	1	–	~5-145	0.26	0.23
2	1	$C_2H_4(OH)_2$	~5-150	0.36	0.16
3	1.5	$C_2H_4(OH)_2$	~20-185	0.33	0.26

Table 6 Magnetic characteristics in the field of 1270 kA/m of $YFe_{1-x}Ni_xO_3$ nanopowders (x = 0.1; 0.15; 0.3) after thermal annealing at 800°C, 60 min, measured at 100 and 300 K

№	G/N	Gelling agents	Particle size (TEM), nm	J(300K), A·m²/kg	J(100K), A·m²/kg
6	1	–	5-100	0.066	0.145
8	1.5	$C_3H_5(OH)_3$	5-35	0.1	0.09
9	2	$C_3H_5(OH)_3$	4-55	0.128	0.133
10	1.5	$C_2H_4(OH)_2$	5-50	0.056	0.42
11	2	$C_2H_4(OH)_2$	4-70	0.176	0.092

doping) under the conditions of a self-propagating wave of glycine-nitrate combustion in the region of the stoichiometric parameter G/N from 1 to 2, materials that exhibit different magnetic properties were formed. Fine adjustment of the magnetic characteristics by changing the G/N ratio of components and using various gelling agents in the synthesis of nanocrystals is possible.

4. Conclusions

Yttrium orthoferrite nanocrystals (with and without doping) were synthesized under glycine–nitrate combustion conditions at G/N = 1 and 1.5 without adding a gelling agent to the reaction mixture and using ethylene glycol/glycerol. It was established that thermal annealing for an hour at 800 °C led to the formation of the main phase of o-$YFeO_3$. For undoped yttrium orthoferrite samples, a particle diameter of the order of 5–185 nm was characteristic, depending on the gelling agent (TEM) used. The study of the magnetic characteristics demonstrated that $YFeO_3$ samples, synthesized with the use of ethylene glycol as a gelling agent, were characterized by antiferromagnetic behaviour up to extremely low temperatures (below 2 K), and the use of glycerol as a gelling agent in a similar process led to the formation of particles with an uncompensated magnetic moment, most probably caused by the weak ferromagnetism of yttrium ferrite, which exhibits a magnetically hard response. In the case of yttrium orthoferrite doped with Ni^{2+}, under the same conditions, particles were characterized by a predominantly rounded shape with a size of 24 to 31 nm (TEM). Changes in the magnetic properties of $YFeO_3$ nanocrystalline powders doped with nickel was due to the incorporation of Ni^{2+} ($r(Ni^{2+})$ = 0.69 Å) in the position of Fe^{3+} ($r(Fe^{3+})$ = 0.645 Å), which led to the formation of a material with more expressed soft magnetic properties at a degree of substitution of 0.1. Samples with higher degrees of substitution also exhibited paramagnetic behaviour at temperatures above 100 K.

Author contributions

The authors contributed equally to this article.

Conflict of interests

The authors declare that they have no known competing financial interests or personal relationships that could have influenced the work reported in this paper.

References

1. Saukhimov A. A., Hobosyan M. A., Dannangoda G. C., Zhumabekova N. N., Almanov G. A., Kumekov S. E., Martirosyan K. S. Solution-combustion synthesis and magnetodielectric properties of nanostructured rare earth ferrites. *International Journal of Self-Propagating High-Temperature Synthesis*. 2015;24(2): 63–71. https://doi.org/10.3103/S1061386215020065

2. Popkov V. I., Almjasheva O. V., Gusarov V. V. The investigation of the structure control possibility of nanocrystalline yttrium orthoferrite in its synthesis from amorphous powders. *Russian Journal of Applied Chemistry*. 2014;87(10): 1417–1421. https://doi.org/10.1134/S1070427214100048

3. Nguyen A. T., Nguyen V. Y., Mittova I. Ya., Mittova V. O., Viryutina E. L., Hoang C. Ch. T., Nguyen Tr. L. T., Bui X. V., Do T. H. Synthesis and magnetic properties of $PrFeO_3$ nanopowders by the co-precipitation method using ethanol. *Nanosystems: Physics, Chemistry, Mathematics*. 2020;11(4): 468–473. https://doi.org/10.17586/2220-8054-2020-11-4-468-473

4. Nguyen A. T., Phan Ph. H. Nh., Mittova I. Ya., Knurova M. V., Mittova V. O. The characterization of nanosized $ZnFe_2O_4$ material prepared by coprecipitation. *Nanosystems: Physics, Chemistry, Mathematics*. 2016;7(3): 459–463. https://doi.org/10.17586/2220-8054-2016-7-3-459-463

5. Sherstyuk D. P., Starikov A. Yu., Zhivulin V. E., Zherebtsov D. A., Gudkova S. A., Perov N. S., Alekhina Yu. A., Astapovich K. A., Vinnik D. A., Trukhanov A. V. Effect of Co content on magnetic features and SPIN states in Ni – Zn spinel ferrites. *Ceramics International*. 2021;47(9): 12163–12169. https://doi.org/10.1016/j.ceramint.2021.01.063

6. Serrao C. R., Sahu J. R., Ramesha K., Rao C. N. R. Magnetoelectric effect in rare earth ferrites, $LnFe_2O_4$. *Journal of Applied Physics*. 2008;104(1): 16102. https://doi.org/10.1063/1.2946455

7. Xu C., Yang Y., Wang S., Duan W., Gu B., Bellaiche L. Anomalous properties of hexagonal rare-earth ferrites from first principles. *Physical Review B*. 2014;89: 205122. https://doi.org/10.1103/PhysRevB.89.205122

8. Kanhere P., Chen Z. A review on visible light active perovskite-based photocatalysts. *Molecules*. 2014;19: 19995–20022. https://doi.org/10.3390/molecules191219995

9. Ahmad T., Lone I. H., Ansari S. G., Ahmed J., Ahamad T., Alshehri S. M. Multifunctional properties and applications of yttrium ferrite nanoparticles prepared by citrate precursor route. *Materials and Design*. 2017;126: 331–338. https://doi.org/10.1016/j.matdes.2017.04.034

10. Jabbarzare S., Abdellahi M., Ghayour H., Chami A., Hejazian S. Mechanochemically assisted synthesis of yttrium ferrite ceramic and its visible light photocatalytic and magnetic properties. *Journal of Alloys and Compounds*. 2016;688: 1125–1130. https://doi.org/10.1016/j.jallcom.2016.07.123

11. Suthar L., Bhadala F., Roy M. Structural, electrical, thermal and optical properties of $YFeO_3$, prepared by SSR and sol – gel route: a comparative study. *Applied Physics A*. 2019;125: 452. https://doi.org/10.1007/s00339-019-2743-1

12. Nguyen A. T., Pham V. N. T., Nguyen T. T. L., Mittova V. O., Vo Q. M., Berezhnaya M. V., Mittova I. Ya., Do Tr. H., Chau H. D. Crystal structure and magnetic properties of perovskite $YFe_{1x}Mn_xO_3$ nanopowders synthesized by co-precipitation method. *Solid State Sciences*. 2019;96: 105922. https://doi.org/10.1016/j.solidstatesciences.2019.06.011

13. Popkov V. I., Almjasheva O. V. Formation mechanism of $YFeO_3$ nanoparticles under the hydrothermal condition. *Nanosystems: Physics, Chemistry, Mathematics*. 2014;5(5): 703–708. Available at: https://www.elibrary.ru/item.asp?id=22415667

14. Berezhnaya M. V., Al'myasheva O. V., Mittova V. O., Nguyen A. T., Mittova I. Ya. Sol-gel synthesis and properties of $Y_{1-x}Ba_xFeO_3$ nanocrystals. *Russian Journal of General Chemistry*. 2018;88(4): 626-631. https://doi.org/10.1134/S1070363218040035

15. Popkov V. I., Almjasheva O. V., Semenova A. S., Kellerman D. G., Nevedomskiy V. N., Gusarov V. V. Magnetic properties of $YFeO_3$ nanocrystals obtained by different soft-chemical methods. *Journal of Materials Science: Materials in Electronics*. 2017;28; 7163–7170. https://doi.org/10.1007/s10854-017-6676-1

16. Shobana M. K., Kwon H., Choe H. Structural studies on the yttrium-doped cobalt ferrite powders synthesized by sol-gel combustion method. *Journal of Magnetism and Magnetic Materials*. 2012;324: 2245–2248. https://doi.org/10.1016/j.jmmm.2012.02.110

17. Nguyen T. A., Pham V. N. T., Le H. T., Chau D. H., Mittova V. O., Nguyen L. T. Tr., Dinh D. A., Nhan Hao T. V., Mittova I. Ya. Crystal structure and magnetic properties of $LaFe_{1x}Ni_xO_3$ nanomaterials prepared via a simple co-precipitation method. *Ceramics International*. 2019;45: 21768–21772. https://doi.org/10.1016/j.ceramint.2019.07.178

18. Lima E., De Biasi E., Mansilla M. V., Saleta M. E., Granada M., Troiani H. E., Rechenberg H. R., Zysler R.D. Heat generation in agglomerated ferrite nanoparticles in an alternating magnetic field. *Journal of Physics D: Applied Physics*. 2012;46: 045002. https://doi.org/10.1088/0022-3727/46/4/045002

19. Bachina A., Ivanov V. A., Popkov V. I. Peculiarities of $LaFeO_3$ nanocrystals formation via glycine-nitrate combustion. *Nanosystems: Physics, Chemistry, Mathematics*. 2017;8(5): 647–653. https://doi.org/10.17586/2220-8054-2017-8-5-647-653

20. Martinson K. D., Kondrashkova, I. S., Popkov V. I. Synthesis of $EuFeO_3$ nanocrystals by glycine-nitrate combustion method. *Russian Journal of Applied Chemistry*. 2017;90(8): 1214–1218. https://doi.org/10.1134/S1070427217080031

21. Popkov V. I., Almjasheva O. V., Nevedomskyi V. N., Panchuk V. V., Semenov V. G., Gusarov V. V. Effect of spatial constraints on the phase evolution of $YFeO_3$-based nanopowders under heat treatment of glycine-nitrate combustion products. *Ceramics International*. 2018;44: 20906–20912. https://doi.org/10.1016/j.ceramint.2018.08.097

22. Lebedev L. A., Tenevich M. I., Popkov V. I. The effect of solution-combustion mode on the structure, morphology, and size-sensitive photocatalytic performance of $MgFe_2O_4$ nanopowders. *Condensed Matter and Interphases*. 2022;24(4): 496–503. https://doi.org/10.17308/kcmf.2022.24/10645

23. Popkov V. I., Almjasheva O. V., Nevedomskiy V. N., Sokolov V. V., Gusarov V. V. Crystallization behavior and morphological features of $YFeO_3$ nanocrystallites obtained by glycine-nitrate combustion. *Nanosystems: Physics, Chemistry, Mathematics*. 2015;6(6): 866–874. https://doi.org/10.17586/2220-8054-2015-6-6-866-874

24. Popkov V. I., Almyasheva O. V. Yttrium orthoferrite nanopowders formation under glycine-nitrate combustion conditions. *Journal of Applied Chemistry*. 2014;87(2): 167–171. https://doi.org/10.1134/S1070427214020074

25. Nguyen A. T., Chau H. Nguyen A. T., Chau H. O., Huong D. T., Mittova I. Ya. Structural and magnetic properties of $YFe_{1-x}Co_xO_3$ ($0.1<x<0.5$) perovskite nanomaterials synthesized by coprecipitation method. *Nanosystems: physics, chemistry, mathematics*. 2018;9(3): 424–429. https://doi.org/10.17586/2220-8054-2018-9-3-424-429

26. Nguyen A. T., Mittova I. Ya., Solodukhin D. O., Al'myasheva O. V., Mittova V. O., Demidova S. Yu. Sol-gel formation and properties of nanocrystals of solid solutions $Y_{1x}Ca_xFeO_3$. *Journal of Inorganic Chemistry*. 2014;59(2): 40–45. https://doi.org/10.7868/S0044457X14020159

27. Pomiro F., Gil D. M., Nassif V., Paesano A., Gomez M. I., Guimpel J., Sanchez R. D., Carbonio R. E. Weak ferromagnetism and superparamagnetic clusters coexistence in $YFe_{1x}co_xO_3$ ($0 \leqslant x \leqslant 1$) perovskites. *Materials Research Bulletin*. 2017;94: 472–482. https://doi.org/10.1016/j.materresbull.2017.06.045

28. Tomina E. V., Kurkin N. A., Maltsev S. A. Microwave synthesis of yttrium orthoferrite and doping with nickel. *Condensed Matter and Interphases*. 2019;21(2): 306–312. https://doi.org/10.17308/kcmf.2019.21/768

29. Tomina E. V., Darinsky B. M., Mittova I. Ya., Churkin V. D., Boikov N. I., Ivanova O. B. Microwave-assisted synthesis of $YCo_xFe_{1-x}O_3$ nanocrystals. *Inorganic materials*. 2019;55(4): 390–394. https://doi.org/10.1134/S0002337X19040158

30. Shannon R.D. Revised effective ionic radii and systematic studies of interatomic distances in halides and chalcogenides. *Acta Crystallographica Section A*. 1976; A32(5): 751–767. https://doi.org/10.1107/S0567739476001551

31. Nguyen A. T., Pham V., Chau D. H., Mittova V. O., Mittova I. Ya., Kopeychenko E. Nguyen A. T., Pham V., Chau D. X., Nguyen A.T. P. Effect of Ni substitution on phase transition, crystal structure and magnetic properties of nanostructured $YFeO_3$ perovskite. *Journal of Molecular Structure*. 2020;1215: 12829. https://doi.org/10.1016/j.molstruc.2020.128293

32. Berezhnaya M. V., Mittova, I. Ya., Perov N. S., Al'myasheva O. V., Nguyen A. T., Mittova V. O., Bessalova V. V., Viryutina E. L. Production of zinc-doped yttrium ferrite nanopowders by the sol-gel method. *Russian Journal of Inorganic Chemistry*. 2018;63(6): 742–746. https://doi.org/10.7868/S0044457X18060077

Author information

Evgenia I. Lisunova, PhD student of the Department of Materials Science and the Industry of Nanosystems, Voronezh State University (Voronezh, Russian Federation).
https://orcid.org/0000-0002-8657-2135
kopejchenko00@mail.ru

Nikolai S. Perov, Dr. Sci. (Phys.–Math.), Professor, Head of the Department of Magnetism, Faculty of Physics, Lomonosov Moscow State University (Moscow, Russian Federation).
https://orcid.org/0000-0002-0757-4942
perov@magn.ru

Valentina O. Mittova, PhD, Professor of the Scientific-Research Institute of Experimental and Clinical Medicine, Laboratory of Molecular Medicine, Teaching University Geomedi (Tbilisi, Georgia).
https://orcid.org/0000-0002-9844-8684
valentina.mittova@geomedi.edu.ge

Boris V. Sladkopevtsev, Cand. Sci. (Chem.), Associate Professor of the Department of Materials Science and Nanosystem Technologies, Voronezh State University (Voronezh, Russian Federation).
https://orcid.org/0000-0002-0372-1941
dp-kmins@yandex.ru

Xuan Vuong Bui, PhD in Chemistry, Lecturer of the Faculty of Natural Sciences Education, Saigon University (Ho Chi Minh City, Vietnam).
https://orcid.org/0000-0002-3757-1099
bxvuong@sgu.edu.vn

Anh Tien Nguyen, PhD in Chemistry, Chief of Inorganic Chemistry Department, Ho Chi Minh City University of Education (Ho Chi Minh City, Vietnam).
https://orcid.org/0000-0002-4396-0349
tienna@hcmue.edu.vn

Yulia A. Alekhina, Researcher of the Department of Magnetism, Faculty of Physics, Lomonosov Moscow State University n (Moscow, Russian Federation).
https://orcid.org/0000-0003-1776-5782
Ya.alekhina@physics.msu.ru

Viktor F. Kostryukov, Dr. Sci. (Chem.), Associate Professor, Associate Professor of the Department of Materials Science and the Industry of Nanosystems, Voronezh State University (Voronezh, Russian Federation).
https://orcid.org/0000-0001-5753-5653
vc@chem.vsu.ru

Irina Ya. Mittova, Dr. Sci. (Chem.), Professor of the Department of Materials Science and the Industry of Nanosystems, Voronezh State University (Voronezh, Russian Federation).
https://orcid.org/0000-0001-6919-1683
imittova@mail.ru

Received 30.08.2022; approved after reviewing 12.09.2023; accepted for publication 15.09.2022; published online 25.03.2023.

Translated by Valentina Mittova
Edited and proofread by Simon Cox